Levoglucosenone-derived monomers for sustainable polymers: From biomass conversion to functional materials

Guangke Wang , Shihao Ji , Zi-Chen Li , Changxia Shi

PII: S1001-8417(26)00224-X
DOI: https://doi.org/10.1016/j.cclet.2026.112581
Reference: CCLET 112581

To appear in: *Chinese Chemical Letters*

Please cite this article as: Guangke Wang , Shihao Ji , Zi-Chen Li , Changxia Shi , Levoglucosenone-derived monomers for sustainable polymers: From biomass conversion to functional materials, *Chinese Chemical Letters* (2026), doi: https://doi.org/10.1016/j.cclet.2026.112581

Review

Levoglucosenone-derived monomers for sustainable polymers: From biomass conversion to functional materials

Guangke Wang[a,b,1], Shihao Ji[b,1], Zi-Chen Li[a,*], Changxia Shi[b,*]

[a] *Beijing National Laboratory for Molecular Sciences, Key Laboratory of Polymer Chemistry and Physics of Ministry of Education, Center for Soft Matter Science and Engineering, College of Chemistry & Molecular Engineering, Peking University, Beijing 100871, China*

[b] *Beijing National Laboratory for Molecular Sciences, Laboratory of Polymer Physics and Chemistry, Institute of Chemistry, Chinese Academy of Sciences, Beijing 100190, China*

ARTICLE INFO

Article history:
Received
Received in revised form
Accepted
Available online

Keywords:
Levoglucosenone
Biomass
Sustainable polymers
Functional materials
Ring-opening metathesis polymerization
Cationic ring-opening polymerization

ABSTRACT

Levoglucosenone (LGO) has emerged as a bio-privileged platform molecule at the intersection of biomass valorization and advanced polymer science. Derived from cellulose pyrolysis, LGO possesses a unique combination of structural features, a rigid bicyclic acetal, an *α*,*β*-unsaturated enone, and inherent chirality, that confer exceptional synthetic versatility. Recent advances have established scalable, sustainable routes for LGO production, ranging from acid-catalyzed and ionic liquid-mediated pyrolysis to non-conventional energy-assisted methods and continuous industrial processes. Beyond its synthesis, LGO has been transformed into a broad spectrum of polymer classes *via* diverse methodologies, including ring-opening metathesis polymerization (ROMP), cationic ring-opening polymerization (CROP), radical and controlled radical polymerizations, polycondensation, thiol–ene click chemistry, and direct organobase-catalyzed polymerization. These strategies have yielded polymers spanning rigid high glass transition temperature (T_g) thermoplastics, soft elastomers, degradable networks, and water-soluble macromolecules, thereby illustrating the breadth of LGO's potential as a renewable building block. This review highlights recent advances in LGO synthesis and polymerization, elucidates structure–property relationships, and assesses the prospects of LGO-derived materials within the broader framework of circular and sustainable polymer design.

---

[*] Corresponding authors.
E-mail addresses: zcli@pku.edu (Z.-C. Li), *E-mail address*: cxshi@iccas.ac.edu (C. Shi).

[1] These authors contributed equally to this work.

1. Introduction

The continued dependence of modern society on fossil-based polymers poses acute environmental and socioeconomic challenges, from greenhouse-gas emissions to the escalating accumulation of persistent plastic waste [1-4]. Achieving a sustainable polymer economy [5-8] therefore demands a paradigm shift that integrates sustainability at the molecular-design stage of materials development [9-27]. Central to this transformation is the discovery of renewable monomers that unite scalability, structural diversity, and viable end-of-life (EoL) management within a unified design philosophy [28-37]. Among emerging bio-based [38,39] feedstocks [40-43], levoglucosenone (LGO) occupies a uniquely privileged position [44,45]. Identified originally as a dehydration product of cellulose pyrolysis, LGO is distinguished by a rigid bicyclic framework incorporating a 1,6-anhydro bridge, an *α*,*β*-unsaturated enone, and a well-defined stereocenter [46]. This constellation of features not only imparts stability under processing conditions but also provides multiple reactive handles for selective functionalization and polymerization. As such, LGO has been widely recognized as a gateway molecule bridging lignocellulosic biomass to pharmaceuticals, solvents, and functional polymers [44,46-48].

Over the past decade, significant progress has been made in developing efficient and sustainable synthetic routes to LGO [49]. Classical acid-catalyzed pyrolysis of cellulose remains the benchmark approach, yet innovations such as ionic liquid media, metal-doped catalysts, microwave and plasma-assisted processes, and most notably the industrial Furacell^{TM} continuous pyrolysis platform have addressed challenges of yield, selectivity, and scalability. In parallel, the downstream upgrading of LGO through Baeyer–Villiger oxidation and related transformations has expanded its utility as a precursor to diverse lactones, diols, and fine chemicals [49-54].

The inherent multifunctionality of LGO has also inspired extensive exploration in polymer science [44,47,50]. Depending on the derivatization strategy, LGO can be incorporated into polymers through chain-growth routes (ring-opening metathesis polymerization (ROMP), cationic ring-opening polymerization (CROP), radical polymerization), step-growth condensation (polyesters, hydrazone polymers), thiol–ene network formation, or even direct polymerization of the enone under organobase catalysis. These efforts have produced an array of polymer architectures, from high-performance thermoplastics with glass transitions above 150 °C to elastomers with low-temperature flexibility, and from hydrolytically degradable networks for 3D printing to stereo-regular polysaccharides with recyclability. Such diversity underscores the role of LGO as a platform monomer for sustainable materials design, offering both structural tunability and pathways for circularity.

This review aims to provide a comprehensive overview of the state-of-the-art in LGO chemistry, with a dual focus on: (1) Advances in sustainable and scalable LGO synthesis from lignocellulosic feedstocks and alternative routes, and (2) the development of LGO-derived polymers *via* diverse polymerization methodologies (Fig. 1). By critically evaluating structure–property–function relationships, this review seeks to position LGO at the forefront of renewable monomer research and to outline future opportunities for integrating LGO into next-generation sustainable polymer technologies.

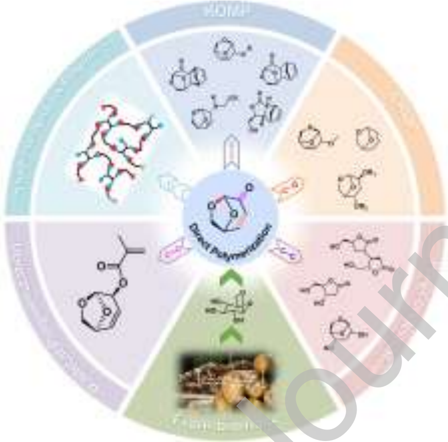

Fig. 1. Structural overview of LGO-derived monomers and polymerization pathways.

2. Synthesis and preparation strategies

2.1. Synthetic strategies toward LGO

LGO, most commonly produced *via* cellulose pyrolysis, has been recognized as a bio-privileged platform molecule owing to its rigid bicyclic acetal and electron-deficient *α*,*β*-unsaturated enone functionalities [55,56]. These distinctive structural features confer inherent chirality, stability, and synthetic versatility, making LGO a valuable intermediate for pharmaceuticals, green solvents such as Cyrene^{TM}, and bio-based polymers. Over recent decades, a variety of strategies for LGO production have been developed, ranging from classical acid-catalyzed pyrolysis of cellulose to more advanced catalytic, ionic-liquid mediated, and non-conventional energy-assisted approaches [57-71]. Together, these efforts have significantly advanced the scalability and sustainability of LGO synthesis, consolidating its role as a cornerstone in the valorization of renewable feedstocks.

Historically, LGO was first identified in the early 1970s as a major product of acid-catalyzed pyrolysis of cellulose [72], and subsequently characterized in detail by Shafizadeh and coworkers (Fig. 2) [73]. To complement these pyrolytic studies and expand the accessible feedstocks, several alternative synthetic strategies were later investigated, particularly from 1990s onward, either to probe mechanistic pathways or to access LGO from non-cellulosic precursors. For instance, Shibagaki and co-workers designed an eight-step sequence starting from D-galactose that employed catalytic reductive decarboxylation and afforded LGO in *ca*. 48 % overall yield [74]. Other examples include the dehydration of glucose in the presence of chromium-tanned leather waste, which gave LGO in 12.8 % yield as determined by high-performance liquid chromatography (HPLC), and the enantioselective oxidation of 2-vinylfuran, which provided

LGO with 93 % *ee* after six steps [75,76]. Although conceptually elegant, these approaches generally rely on costly feedstocks, multistep sequences, or toxic reagents, and therefore remain impractical for large-scale application.

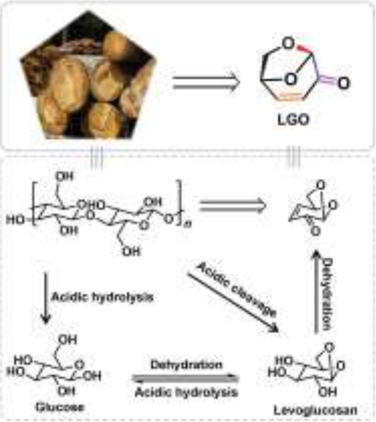

Fig. 2. Schematic illustration of the conversion of biomass-derived cellulose to LGO *via* acidic hydrolysis, cleavage, and dehydration pathways.

By contrast, practical development of LGO has relied on the classical acid-catalyzed dehydration of cellulose, in which mineral acids such as sulfuric acid or phosphoric acid in polar aprotic solvents (*e.g.*, tetrahydrofuran (THF), γ-valerolactone) promote cleavage of glycosidic bonds and subsequent intramolecular rearrangement [77]. Selectivities of up to 95 % have been reported under dilute conditions (typically 1–2 wt% cellulose in 1,4-dioxane at 160–200 °C), but the overall isolated yields remain modest [78]. To improve performance, cellulose impregnated with phosphoric acid has been subjected to catalytic fast pyrolysis at 200–250 °C, yielding approximately 18 wt% LGO [79]. Similarly, phosphoric acid-activated carbon has been shown to enhance selectivity of liquid products to *ca*. 76 % [80].

Subsequent developments introduced heterogeneous catalysts to improve yield, selectivity, and recyclability. Mesoporous silicates such as Ni–P–MCM-41 and Al–MCM-41, afforded LGO in 20–21 wt% yield [81]. Nanostructured oxides including TiO_2, Al_2O_3, and mixed Al–Ti oxides achieved comparable yields of up to 22 wt% [82]. More recently, magnetic solid acid catalysts such as Fe_3O_4/$CeSO_3H$ have been introduced to facilitate recovery and recycling, though gradual deactivation remains a limitation [83]. In parallel, alternative solvent systems, in particular ionic liquids (ILs), have also been explored to reduce reliance on corrosive mineral acids. Sulfonated imidazolium salts at 180–220 °C enabled yields of ~30 wt% LGO, and supported IL phases have been integrated into continuous-flow pyrolysis, affording ~25 wt% yield with partial solvent recyclability [84]. In some cases, the system could be directly coupled with downstream hydrogenation to Cyrene^{TM}, highlighting process intensification opportunities [57]. However, the trade-off between ILs recovery efficiency and product yield is yet to be resolved. Non-conventional energy inputs provide additional process intensification options. Microwave-assisted pyrolysis, for example, has been carried out in the presence of clays at 180–200 °C, producing LGO in ~12 wt% yield with purities up to 63 % [85]. Plasma-assisted electrolysis has achieved considerably higher yields of up to 43 % under mild temperatures (<180 °C), while reducing energy consumption by more than 70 % relative to conventional heating. Despite their promise, neither technology has yet been demonstrated at pilot or industrial scale [86].

Finally, direct conversion of lignocellulosic biomass, bypassing the need for purified cellulose, has been examined. Microwave-assisted pyrolysis of lignin-rich agricultural waste streams afforded LGO in ~8 wt% yield, while extruder-based catalytic fast pyrolysis of sawdust, as implemented in Circa's Furacell^{TM} process, remains the only commercially validated technology. This continuous process operates under acid catalysis at 200–250 °C and has achieved production at the 50 t/year scale, with expansion targets exceeding 1000 t/year [42].

Taken together, while total synthesis routes provide mechanistic insights, they remain impractical for large-scale application. In contrast, acid-catalyzed pyrolysis and catalytic biomass conversion continue to represent the most promising strategies, with the Furacell^{TM} process standing as the sole industrially demonstrated technology [87]. Looking forward, advances in catalyst stability and recyclability, solvent sustainability, and energy efficiency will be critical to consolidate LGO production as a cornerstone of the emerging bio-based chemical industry [45].

2.2. LGO derivatization and polymerization pathways

Although LGO possesses highly reactive functionalities, its direct polymerization is intrinsically challenging. The rigid bicyclic acetal framework restricts chain propagation, while the electron-deficient α,β-unsaturated enone moiety tends to undergo competing side reactions such as Michael addition, crosslinking, or degradation rather than controlled chain growth. As a result, only a few attempts have been successful in the translating native LGO directly into polymers, and most advances have focused on transforming LGO into reactive intermediates or monomers compatible with established polymerization mechanisms.

2.2.1. Direct polymerization of native LGO

A recent breakthrough demonstrated that LGO itself can serve as a polymerizable substrate without prior derivation. Pollard, Banwell, and Connal reported an unprecedented direct polymerization of LGO *via* a DBU-catalyzed Rauhut–Currier-type process, in which the enone moiety undergoes intermolecular conjugate additions, regenerating the alkene functionality and thereby enabling chain propagation (Fig. 3) [88]. Optimized reactions in polar aprotic solvents (notably dichloromethane (DCM)) at 90 °C yielded polymers with M_n up to 278 kDa ($Đ \approx 3.9$) after 21 h, and as high as 246 kDa at extended reaction times, representing the most atom-economical route to LGO-based polymers reported to date (atom economy ~99 %, E-factor 0.012).

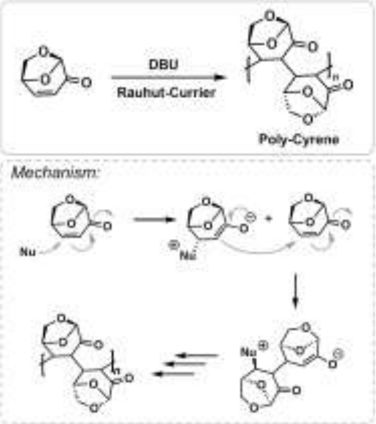

Fig. 3. Rauhut–Currier-type polymerization mechanism for converting LGO into poly-Cyrene.

The resulting "poly-Cyrene" exhibited excellent thermal stability, with $T_{d,5\,\%}$ (temperature at 5 % mass loss) ≈ 249 °C and $T_{d,50\,\%}$ (temperature at 5 % mass loss) > 400 °C, but no discernible T_g below its decomposition temperature. The polymers were soluble in polar solvents such as dimethyl sulfoxide (DMSO) (up to 450 g/L) and could be cast into brittle, reflective films, although mechanical robustness was limited. Importantly, further Baeyer–Villiger oxidation of poly-Cyrene in aqueous H_2O_2 at 50 °C converted the hydrophobic scaffold into a hydrophilic poly-2H-HBO, with enhanced solubility in water (~850 mg/mL) while maintaining high thermal stability ($T_{d,5\,\%}$ = 265 °C).

This study underscores the unique feasibility of direct biomass-to-polymer conversion from LGO, providing a scalable, atom-efficient route that bypasses monomer derivatization. Nonetheless, the lack of control over molar mass distribution and limited mechanical performance underscore why most subsequent efforts have shifted toward LGO derivatization strategies. By modifying the enone, ketal, or hydroxyl functionalities, LGO can be transformed into monomers amenable to ring-opening, radical, condensation, or click-type polymerizations. This approach not only circumvents the reactivity issues of native LGO but also introduces functional handles that tailor the resulting polymers' thermal, mechanical, and degradative properties. As such, LGO serves less as a "ready-to-polymerize" monomer and more as a versatile precursor to a family of functional building blocks that can be incorporated into diverse polymer architectures.

2.2.2. LGO-derived monomers for ROMP: From synthetic strategies to functional polymers

Among the derivatization-based approaches, ROMP has emerged as a particularly effective strategy, enabling access to high-performance polymers with tunable thermal stability, degradability, and functionalization potential. The key lies in overcoming the poor reactivity of native LGO, where the electron-deficient enone adjacent to the olefin deactivates Ru catalysts.

Early work by Schlaad and co-workers demonstrated that quantitative reduction of LGO to levoglucosenol (LGOH) removed the problematic carbonyl group, rendering the strained internal double bond suitable for ROMP (Fig. 4) [89]. Using a mono-ortho-substituted NHC Ru catalyst, they achieved conversions of 50 %–60 % in 1,4-dioxane, producing polymers with M_n up to 100 kDa, albeit under narrow temperature and concentration windows and with non-living characteristics. The resulting poly(LGOH) was soluble in polar solvents, thermally stable up to ~220 °C, and displayed a high T_g of ~100 °C. Acid-catalyzed depolymerization in dioxane demonstrated intrinsic chemical recyclability.

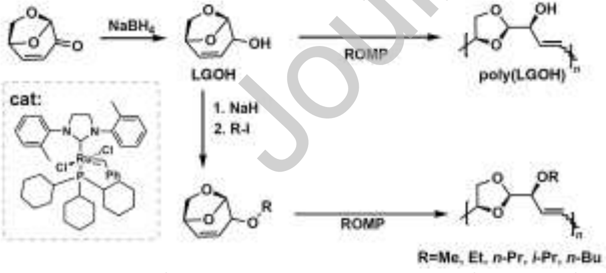

Fig. 4. Synthesis of LGOH and its *O*-alkyl derivatives from LGO, followed by ROMP using a Ru-based Grubbs catalyst to afford the corresponding polymers.

Further solubility tuning was achieved by Schlaad and co-workers through simple etherification of LGOH to yield levoglucosenyl alkyl ethers (Fig. 4) [90]. Their ROMP produced amorphous thermoplastics with T_g ranging from ~43 °C (Me) to 0 °C (*n*-Bu) and thermal stability up to 285 °C. This work highlighted how subtle side-chain variations can modulate both solubility and thermomechanical properties.

Structural diversification *via* Diels–Alder adducts of LGO with cyclopentadiene provided norbornene-type monomers (endo/exo-*N*-LGO) and their oxidized analogue (*N*-HBO) (Fig. 5) [91]. ROMP of these strained bicyclic derivatives with first-generation Grubbs catalysts afforded polymers with high conversions (up to 98 %), M_n up to 122 kDa and remarkable thermostability with $T_{d,5\,\%}$ of 336–380 °C). Copolymerization and post-polymerization Baeyer–Villiger oxidation further broadened tunability.

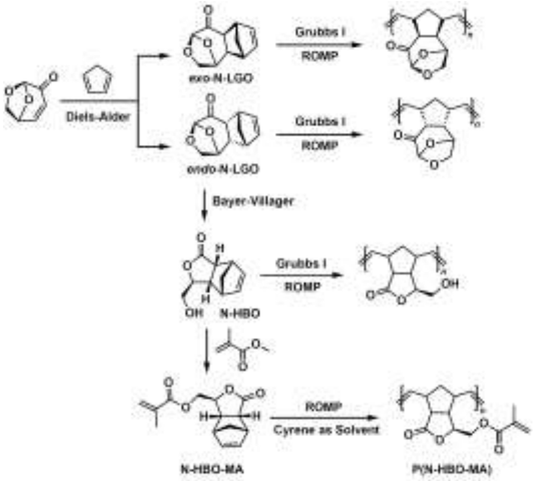

Fig. 5. ROMP of LGO-derived bicyclic to afford structurally varied norbornene-based polymers.

Allais and co-workers advanced this concept by designing a bifunctional monomer (*N*-HBO-MA) bearing both norbornene and methacrylate groups *via* chemo-enzymatic synthesis [92]. Selective ROMP of the norbornene moiety in bio-based Cyrene^{TM} solvent afforded well-defined polymers with M_n up to 264 kDa and exceptional thermostability ($T_{d,5\,\%} \approx 400$ °C). Pendant methacrylates enabled further functionalization, illustrating how enzyme-mediated derivatization and green solvents can synergistically enhance sustainability.

Banwell and co-workers explored Diels–Alder adducts from both LGO and isoLGO, producing highly strained bicyclic monomers with six stereocenters (Fig. 6) [93]. ROMP using third-generation Grubbs catalysts achieved living character, predictable M_n up to ~85 kDa, and enabled pseudoenantiomeric block copolymers. Post-modifications (reduction, etherification, fluorination) yielded polymers with diverse functionalities, solubilities, and optical activities, underscoring the stereochemical richness of LGO-derived monomers.

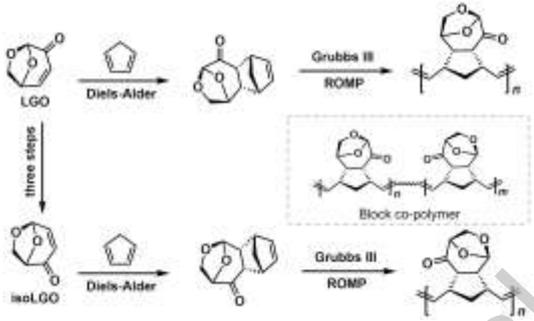

Fig. 6. ROMP of Diels–Alder adducts derived from LGO and isoLGO affords homochiral polymers and block copolymers.

Recent breakthroughs have addressed long-standing issues of poor reactivity and uncontrolled kinetics. Choi and co-workers developed cascade enyne monomers that underwent controlled ROMP with third-generation Grubbs catalysts, yielding polymers with M_n up to 65 kDa, $Đ = 1.06–1.25$, and exceptionally high T_g (152–198 °C) while retaining acid degradability (Fig. 7) [94]. Independently, Gutekunst and co-workers designed alkyne-functionalized LGO enyne monomers, achieving living polymerizations with M_n up to 59 kDa, low $Đ$, and amphiphilic block copolymers forming micelles. Their acid-labile backbones enabled clean depolymerization, establishing a versatile route to degradable thermoplastics and functional biomaterials [95].

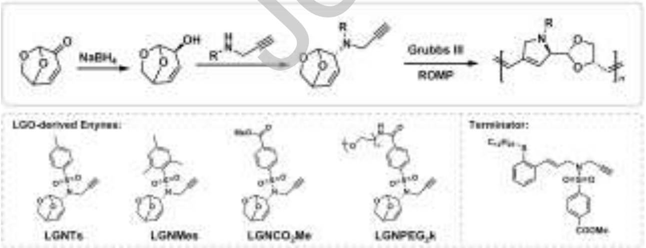

Fig. 7. Controlled cascade ROMP of enyne monomers derived from LGO affords degradable thermoplastics and functional polymers.

In summary, ROMP has evolved from modest successes with reduced LGOH to a broad platform of functionalized derivatives, including norbornene, enyne, and bifunctional monomers, that provide access to high-molecular-weight, thermostable, and in many cases chemically recyclable polymers. The ability to incorporate stereochemical information, reactive side groups, and degradable linkages underscores the unique promise of ROMP in valorizing LGO as a renewable monomer platform.

2.2.3. CROP of LGO-derived monomers

CROP provides an attractive route to access acetal-based polymers from LGO derivatives, combining semicrystallinity, degradability, and versatile post-functionalization. However, the intrinsic electron-deficient enone of LGO and the poor reactivity of LGOH toward cationic conditions have necessitated derivatization to more suitable substrates.

Schlaad and co-workers demonstrated the first CROP of an LGO derivative by methylating LGOH to give Levoglucosenyl methyl ether (LGO-Me) (Fig. 8) [96]. Polymerization with strong Lewis or Brønsted acids (*e.g.*, $BF_3 \cdot OEt_2$, TfOH) afforded semicrystalline polyacetals (M_n up to ~36 kDa, $Đ \approx 1.4$) with $T_g \approx 35$ °C and thermal stability to ~220 °C. Retained pendant olefins allowed crosslinking, thiol–ene additions, and hydrogenation, while the polymers degraded rapidly under acid/methanol, confirming their acid-labile nature. This established CROP of LGO derivatives as a straightforward entry to degradable, functional polyacetals.

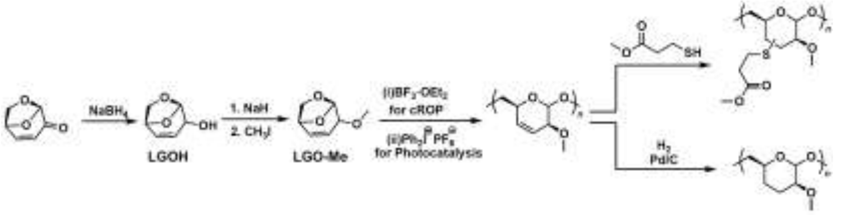

Fig. 8. CROP of the LGO-derived cyclic acetal (LGO-Me) yields a polyacetal that is amenable to further chemical modification.

Building upon this, Schlaad and Yagci developed a photoinduced variant (photo-CROP) of LGO-Me, using diphenyliodonium salts as photoacid generators under UV or visible light [97]. The method provided spatiotemporal control, access to significantly higher molar masses (M_n up to 118 kDa at −15 °C), and evidence of living characteristics, as shown by successful block copolymer synthesis with vinyl ethers. The resulting polymers exhibited sharp melting transitions (90–150 °C) and enhanced thermal stability (~250 °C). Compared to thermally initiated systems, photo-CROP offered an energy-efficient route that combines control, scalability, and compatibility with visible light initiators, highlighting its potential for green macromolecular engineering.

Reineke and Ellison later expanded the scope to cationic ring-opening copolymerization (CROCOP) of levoglucosan derivatives with ε-caprolactone [98]. Using bismuth triflate [$Bi(OTf)_3$] as an efficient and recyclable catalyst, tribenzyl- and triallyl-protected levoglucosan were copolymerized to produce well-defined acetal–ester copolymers with M_n up to ~15 kDa and narrow $Đ$. By adjusting the feed ratio, the levoglucosan incorporation could be systematically tuned (16–79 %), which translated into a wide range of thermal properties: T_g values from −44 °C to +34 °C and crystalline melting transitions arising from the caprolactone-rich segments. Importantly, the allyl-protected systems retained pendant C=C bonds for post-functionalization, creating opportunities for crosslinking or amphiphilic architectures. This study provided the first systematic demonstration that levoglucosan derivatives can be integrated into polyester frameworks, yielding sustainable thermoplastic elastomers and degradable biomaterials.

More recently, Niu and co-workers reported the first living CROP of 1,6-anhydrosugars, a broader class of monomers that includes derivatives of LGO [99]. By employing glycosyl fluoride initiators with $BF_3 \cdot Et_2O$, they achieved controlled chain growth through a reversible activation–deactivation equilibrium, yielding polysaccharides with tunable molecular weights (up to 57 kDa), narrow dispersities, and exclusive α-1,6-glycosidic linkages. These precision polysaccharides were chemically recyclable back to monomer and displayed excellent stability ($T_{d,5\,\%} > 345$ °C), while their morphology and thermal properties could be finely tuned by side-chain substitution. This work represents a milestone in precision glycopolymer synthesis, bridging LGO-derived feedstocks with native-like polysaccharide structures.

Satoh and co-workers further demonstrated that LGO and its hydrogenated derivative Cyrene^{TM} can be converted into bicyclic acetals that undergo efficient CROP to yield unnatural (1→6)-polysaccharides (Fig. 9) [100-103]. These materials combined high thermal stability ($T_{d,5\,\%}$ up to 349 °C), optical transparency, and crucially, closed-loop recyclability: under Brønsted acid catalysis, the polymers depolymerized cleanly to their monomers, which could be re-polymerized without loss of quality. The ability to design tailored substituent patterns (mono- and disubstituted variants) further enabled control over T_g (36–87 °C) and functional handle incorporation.

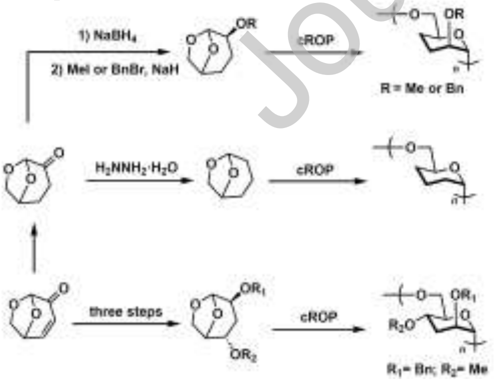

Fig. 9. CROP of LGO-derived “anhydrosugar” monomers bearing different OR substituents to afford polyacetals.

Taken together, these studies underscore the versatility of CROP for valorizing LGO-derived and related anhydrosugar monomers. From semicrystalline polyacetals with pendant functional groups to recyclable, optically transparent polysaccharides, CROP demonstrates how subtle chemical derivatization of LGO can unlock a wide range of controlled, functional, and sustainable polymer architectures.

2.2.4. Radical polymerization of LGO-derived monomers

Radical polymerization has offered versatile entry points into LGO-derived polymers, particularly through methacrylated intermediates that balance synthetic accessibility with reactivity.

Saito and co-workers first developed a bioacrylic monomer from dihydro-5-hydroxy-2(5*H*)-furanone (2*H*-HBO), itself obtained from LGO *via* a green Baeyer–Villiger oxidation [104]. Methacrylation furnished *m*-2*H*-HBO, which retained a pendant lactone ring. This monomer underwent efficient free-radical polymerization in bulk, solution, and emulsion media, as well as controlled reversible addition-fragmentation chain transfer (RAFT) protocols (Fig. 10). While bulk polymerization gave moderate molar masses ($M_n \approx 20$ kDa, $Đ \approx 4.2$, $T_g \approx 95$ °C), emulsion conditions provided higher molar masses ($M_n \approx 25$ kDa), narrower dispersities ($Đ \approx 1.85$), and improved T_g (~108 °C), attributed to micellar confinement. RAFT emulsion polymerization further enabled living characteristics, affording well-defined polymers ($Đ \approx 1.06$) and block copolymers. The resulting poly(*m*-2*H*-HBO) showed high thermal stability ($T_{d,20\,\%} \approx 300$ °C) and poly(methyl methacrylate) (PMMA)-like T_gs (~95–112 °C), underscoring its potential as a renewable substitute for petroleum-based acrylic plastics.

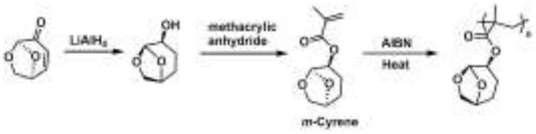

Fig. 10. Synthesis of methacrylated Cyrene™ and its AIBN-initiated radical polymerization.

Building on this concept, the same group reported the first methacrylated derivative of Cyrene™, a commercial solvent derived from LGO [105]. The new monomer (*m*-Cyrene) preserved the bicyclic acetal motif while introducing a polymerizable methacrylate group. Radical polymerizations in bulk, solution, and emulsion all proceeded efficiently, with aqueous emulsions giving the highest molecular weights ($M_n \approx 39$ kDa) and yields (92 %). The resulting polymers combined high T_g (162–192 °C) with excellent thermal stability ($T_{d,20\,\%} \approx 316$ °C), surpassing analogous bio-based methacrylates such as isobutyl methacrylate (IBMA). Reactivity ratio analysis showed high polarity-driven reactivity, while copolymerization studies highlighted compatibility with polar methacrylates but poor incorporation with styrene. Importantly, cytotoxicity assays confirmed non-toxicity, positioning *m*-Cyrene as a safe and scalable alternative for high-performance coatings, adhesives, and engineering plastics.

Most recently, Choi and co-workers achieved the first efficient alternating copolymerization of unmodified LGO with electron-rich dienes *via* RAFT-mediated living radical polymerization (Fig. 11) [106]. Conventional free radical polymerization of LGO or dienes alone was ineffective, but their donor–acceptor pairing enabled efficient propagation. For instance, P(LGO-alt-isoprene) reached $M_n \approx 36.6$ kDa at 73 % conversion, while RAFT control yielded well-defined alternating copolymers ($M_n = 2$–20 kDa, $Đ = 1.1$–1.5). Kinetic and reactivity ratio studies confirmed strongly alternating character ($r_{LGO} = 0.052$, $r_{IP} = 0.028$). The resulting copolymers exhibited robust thermal stability ($T_{d,5\,\%} = 303$–338 °C), tunable T_g values (63–128 °C depending on diene structure), and mechanical performance comparable to polystyrene ($E \approx 2.4$ GPa, $\sigma_B \approx 44$ MPa). Notably, these materials were degradable *via* metathesis catalysis, reverting to defined cyclohexene derivatives, thereby combining precision sequence control with triggered EoL pathways.

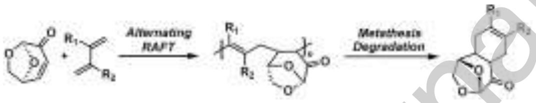

Fig. 11. Alternating RAFT copolymerization of bioderived LGO and dienes.

Collectively, these studies illustrate how radical polymerization can expand the chemical space of LGO-derived monomers. Methacrylation routes yield renewable analogues of commodity acrylics with high thermal robustness, while alternating copolymerization directly incorporates native LGO into degradable, polystyrene-like materials. Together, these approaches establish radical strategies as a powerful complement to ROMP and CROP in valorizing LGO toward scalable, functional, and recyclable polymers.

2.2.5. Polycondensation of LGO- and Cyrene-derived monomers

Polycondensation of LGO- and Cyrene-derived monomers has provided versatile routes to renewable polymers with tunable properties. A notable example is the green Baeyer–Villiger oxidation of LGO and its hydrogenated analogue Cyrene™, which affords the chiral lactone diols (*S*)-*γ*-hydroxymethyl-*α*,*β*-butenolide (HBO) and 2*H*-HBO [107,108]. Using only aqueous hydrogen peroxide as oxidant and solvent, this method avoids metals and organic solvents while operating under mild conditions (50 °C), and has been successfully scaled to kilogram quantities [109]. These enantiopure diols retain the stereocenters of cellulose while introducing reactive lactone motifs, serving as efficient polyester monomers under atom-economical and racemization-free conditions.

Beyond simple lactone diols, more complex diol frameworks have been developed. A sterically hindered bicyclic diol (2*H*-HBO-HBO), obtained *via* dimerization [110] of LGO followed by Baeyer–Villiger oxidation, undergoes polycondensation with diacyl chlorides to give polyesters with M_n up to ~10 kDa (Fig. 12) [111]. The rigid bicyclic architecture imparts high T_g values (up to 81 °C for terephthalate-based analogues, comparable to poly(ethylene terephthalate) (PET)) and excellent thermal stability ($T_{d,50\,\%} = 349$–406 °C). The unsaturated lactone moieties embedded in the backbone also provide sites for post-polymerization functionalization, further broadening the design space.

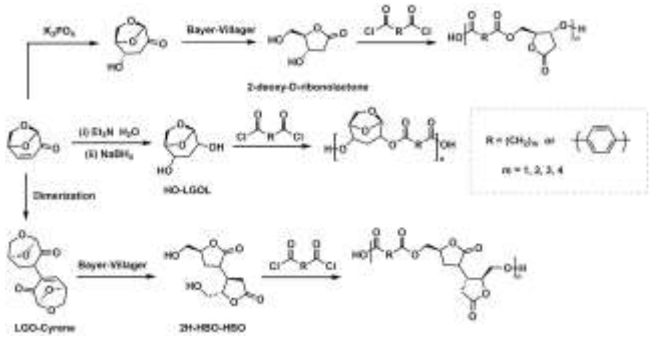

Fig. 12. Preparation of structurally diverse LGO-derived diols and their subsequent polycondensation with diacid chlorides to yield LGO-based polyesters.

Another line of work has focused on cyclic acetal diols [112]. HO-LGOL, synthesized in high yield by hydration–reduction of LGO, was polymerized with diacyl chlorides or diesters to give polyesters with M_n up to 36 kDa, T_g values between 12 °C and 54 °C, and thermal stability above 300 °C (Fig. 12). A life-cycle assessment of different polymerization routes revealed that diester-based polycondensation catalyzed by $Zn(OAc)_2$ was significantly more sustainable than diacyl chloride chemistry, underlining the importance of solvent and catalyst choices in reducing environmental impact. Alternatively, LGO can be treated with K_3PO_4 and subsequently subjected to a Baeyer–Villiger oxidation with H_2O_2 to afford 2-deoxy-D-ribonolactone (Fig. 12), a versatile renewable lactone platform [113]. Condensation of this lactone with aliphatic diacyl chlorides then yields fully bio-based polyesters with tunable thermal properties (T_g = –21 °C to –2 °C; T_m = 87–144 °C).

Structural diversification has also been achieved by introducing pendant terpenoid units. For instance, citronellol was grafted onto LGO through oxa-Michael addition and Baeyer–Villiger oxidation, followed by reduction to yield a triol monomer [114]. Subsequent polycondensation produced branched and crosslinked polyesters with low T_g values (−20 °C to −42 °C) and elastomeric behavior. Enzymatic degradation tests revealed rapid hydrolysis for polymers derived from longer aliphatic diacids, with ~80 % mass loss within 96 h, demonstrating their biodegradability. This contrasts with earlier rigid LGO-based polyesters and illustrates how terpenoid side chains can introduce flexibility, softness, and enzymatic degradability.

By exploiting both the enone and carbonyl moieties, LGO was first converted into bis-thioether intermediates, which were then condensed with dihydrazides to yield bishydrazone-linked polymers [115]. These materials exhibited optical activity, tunable melting points (170–218 °C), and thermal stability up to ~268 °C, while their hydrazone linkages enabled controlled hydrolysis under mild conditions. Unlike conventional polyesters, these polymers degrade in water to defined fragments, providing a rare example of stereo-regular, degradable polycondensates beyond ester backbones.

Taken together, these studies demonstrate that step-growth polymerization of LGO and Cyrene^{TM} derivatives enables access to a wide range of sustainable polymers, from rigid PET-like materials to flexible elastomers and water-degradable biopolymers. The combination of scalable monomer synthesis, structural tunability, and integration of green chemistry principles highlights step-growth strategies as a powerful route for valorizing LGO into advanced, functional condensation polymers.

2.2.6. Thiol–ene network polymers from LGO

Thiol–ene click chemistry has emerged as an effective strategy to convert levoglucosan and LGO derivatives into crosslinked network polymers with tailored mechanical and degradative properties. Porwal, Ellison, and Reineke demonstrated the scalable preparation of levoglucosan-based thiol–ene thermosets using triallyl levoglucosan (TALG) and multifunctional thiols of varying functionality (2SH, 3SH, 4SH, poly3SH) [116]. TALG was obtained in ~80 % yield by mild allylation of levoglucosan, a readily available cellulose pyrolysis product, and the resulting formulations maintained high bio-based content. Photopolymerization monitored by real-time Fourier transform infrared (FTIR) spectroscopy revealed rapid and nearly quantitative consumption of allyl and thiol groups within seconds, yielding gel fractions of 89–97 %. Secondary ene–ene reactions were also observed under irradiation, suggesting that TALG could act as a renewable alternative to conventional reactive diluents such as triallyl isocyanurate or styrene.

The thermosets displayed tunable mechanical properties depending on thiol structure and stoichiometry. At equimolar thiol:ene ratios, tensile strength reached 2.7 MPa, Young’s moduli varied from 3.3 MPa to 14.5 MPa, and elongations at break ranged between 20 % and 35 %. T_gs were typically below room temperature (−27 °C to +7 °C), while thermal stability was excellent with $T_{d,10\,\%}$ above 305 °C. Dynamic mechanical analysis further confirmed adjustable rubbery moduli (2.5–19 MPa) and crosslink densities. Importantly, all networks proved hydrolytically degradable owing to ester linkages: TALG–poly3SH formulations degraded completely within ~50 h in 0.1 mol/L NaOH/THF, whereas TALG–4SH networks required ~7 weeks under similar conditions. Degradation produced soluble alcohols and levoglucosan-derived tricarboxylic acids, eliminating microplastic residues and opening opportunities for chemical feedstock recovery. The potential for practical application was highlighted by direct ink writing 3D printing, where TALG–poly3SH composites printed into complex objects degraded within 30 h in 1 mol/L NaOH, offering a clear EoL pathway for additive manufacturing.

In parallel, Timilsina and Thickett extended thiol–ene chemistry to LGO derivatives, exploiting the unique presence of both internal and terminal alkenes in bifunctional diene monomers synthesized from LGOH (Fig. 13) [117]. Representative derivatives, including an allyl ether and a pentenoate ester, underwent rapid UV-induced thiol–ene polymerization with commercial tetra-thiols, forming transparent crosslinked thermosets. Nuclear magnetic resonance (NMR) studies confirmed that both internal and terminal double bonds participated in thiol–ene addition, though the internal alkenes reacted more slowly. The chemical nature of the linkage exerted a strong influence on network properties: ester-containing monomers polymerized faster and gave stiffer materials, while ether analogues yielded softer, more extensible networks.

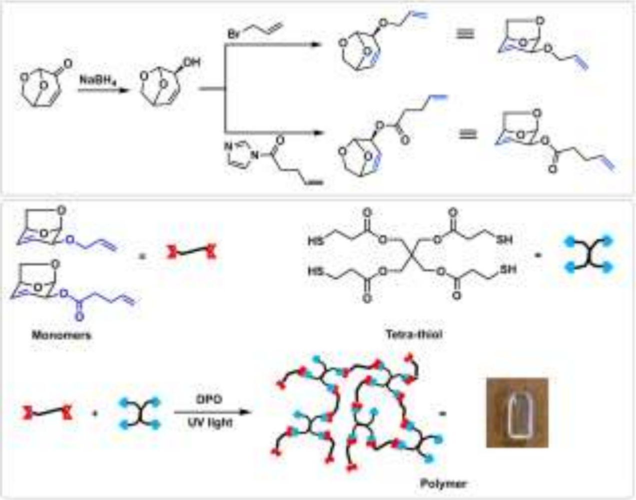

Fig. 13. Thiol–ene photopolymerization of LGO-based ene monomers with a tetrathiol to generate a crosslinked polymer network.

Mechanical testing revealed tensile strengths of 1.3–3.3 MPa, Young's moduli of 0.6–7.8 MPa, and elongations at break ranging from 44 % (ester) to 213 % (ether). T_gs were moderate (23–27 °C), and thermal stability was high with decomposition onset above 320 °C. Solvent-swelling experiments showed good resistance in water and nonpolar media, but rapid disintegration in DCM. Degradation under alkaline conditions confirmed the hydrolytic lability of ester-linked networks, with complete dissolution of ether-rich formulations occurring within five days in 0.5 mol/L NaOH.

Together, these studies highlight the promise of thiol–ene chemistry for transforming levoglucosan and LGO derivatives into renewable, solvent-free, UV-curable thermosets. The ability to fine-tune thermal and mechanical properties through monomer design, combined with hydrolytic degradability and compatibility with advanced processing such as 3D printing, underscores the potential of these systems as sustainable alternatives for coatings, adhesives, and packaging applications.

3. Outlook

The exploration of LGO in polymer science epitomizes the growing paradigm of designing sustainable materials from renewable feedstocks. As a cellulose-derived platform molecule, LGO directly addresses the urgent need to minimize dependence on fossil resources and reduce the carbon footprint of polymer production. Industrial processes such as the Furacell™ continuous pyrolysis route already demonstrate that renewable carbon can be accessed at scale, thereby establishing LGO as a credible entrant in the portfolio of sustainable monomers.

Yet, renewable sourcing alone is not sufficient to secure the future of sustainable polymers. Equally crucial is the integration of built-in functionalities that endow materials with targeted properties while also enabling EoL management. In this regard, LGO offers unique opportunities: its bicyclic acetal framework and *α*,*β*-unsaturated enone allow for tailored derivatization, giving rise to high-T_g thermoplastics, flexible elastomers, water-degradable hydrazone polymers, and hydrolytically degradable networks. These examples underscore that LGO-based polymers are not merely academic curiosities but can deliver practical material properties competitive with, and in some cases superior to, petroleum-based analogues.

Beyond structural diversity, the translation of LGO-derived polymers into real-world applications has gained significant traction. The TALG-based networks have been successfully applied in direct ink writing 3D printing, enabling the fabrication of complex structures such as customized orthopedic implants and microfluidic devices that are capable of complete degradation within 30 h under alkaline conditions, thereby eliminating microplastic waste in additive manufacturing [112]. In parallel, High-T_g thermoplastics, including ROMP-derived enyne polymers (T_g = 152–198 °C) [94] and radical-polymerized *m*-Cyrene polymers (T_g = 162–192 °C) [105], are emerging as sustainable alternatives to petroleum-based engineering plastics for electronic housings, automotive interior components, and aerospace parts, where thermal resistance and mechanical robustness are essential. The PET-like rigid polyesters derived from LGO-based 2H-HBO-HBO further show promise in beverage packaging and textile fibers, matching the performance of conventional polyesters while enabling enzymatic degradation [111]. Additionally, biocompatible and water-soluble LGO-derived polymers such as poly-2H-HBO (water solubility ~850 mg/mL) [88] and citronellol-functionalized elastomeric polyesters [110] are being explored for drug delivery systems, surgical sutures, and temporary wound dressings, leveraging their degradability and low cytotoxicity.

Going forward, a key challenge lies in translating these materials from laboratory demonstrations to scalable applications, which will require close collaboration among Polymer chemists, process engineers, and industry partners. Optimization of processing conditions, such as melt extrusion for thermoplastics, photopolymerization parameters for 3D printing resins, and emulsion polymerization for coating formulations, will be critical to ensuring compatibility with existing manufacturing infrastructure. Moreover, expanding the application scope toward high-value sectors, including controlled drug release systems [95] and high-performance coatings (*e.g.*, non-toxic *m*-Cyrene-based binders for metal substrates [105]), will further unlock new commercial opportunities and accelerate the adoption of LGO-derived sustainable polymers.

Finally, the long-term viability of LGO-derived materials hinges on their contribution to a circular materials economy. Closed-loop recycling or environmentally benign degradation must be considered integral to polymer design. Promising advances already include the acid- or enzyme-triggered depolymerization of LGO-derived polyesters, metathesis-assisted degradation of alternating radical copolymers, and alkaline hydrolysis of thiol–ene thermosets. These proof-of-concept studies highlight pathways by which LGO-based polymers can re-enter the materials cycle either as monomers or as benign degradation products. While Allais *et al*. reported a life cycle assessment (LCA) for their polycondensation system [112], a systematic integration of LCA and techno-economic analysis (TEA) into polymer design remains essential to rigorously benchmark environmental benefits and inform scalable implementation.

In summary, the future of LGO-derived polymers will be determined by the convergence of three pillars: (1) Renewable feedstocks, ensuring low-carbon sourcing; (2) built-in functionalities, providing competitive and application-relevant material properties; and (3) circular regeneration pathways, enabling recyclability and degradability by design. Advancing along these lines will not only consolidate LGO as a cornerstone of bio-based monomer chemistry but also contribute to the broader realization of truly sustainable polymers.

Declaration of competing interest

The authors declare that they have no known competing financial interests or personal relationships that could have appeared to influence the work reported in this paper.

Acknowledgments

This work was supported by the Strategic Priority Research Program of the Chinese Academy of Sciences (No. XDA0540000), Advanced Materials-National Science and Technology Major Project (No. 2025ZD0615001), National Natural Science Foundation of China (No. 52503014), Chinese Academy of Sciences.

References

[1] J.R. Jambeck, R. Geyer, C. Wilcox, et al., Science 347 (2015) 768-771.
[2] R. Geyer, J.R. Jambeck, K.L. Law, Sci. Adv. 3 (2020) e1700782.
[3] S.B. Borrelle, J. Ringma, K.L. Law, et al., Science 369 (2020) 1515-1518.
[4] P. Stegmann, V. Daioglou, M. Londo, et al., Nature 612 (2022) 272-276.
[5] J. Chen, W. Wang, C. Zou, et al., J. Am. Chem. Soc. 147 (2025) 24747-24758.
[6] W. Li, D. Liao, Y. Li, et al., Sci. China Chem. 68 (2025) 2589-2594.
[7] G. Si, C. Li, M. Chen, et al., Angew. Chem. Int. Ed. 62 (2023) e202311733.
[8] C. Zou, J. Chen, M.A. Khan, et al., J. Am. Chem. Soc. 146 (2024) 19449-19459.
[9] M. Hong, E.Y.X. Chen, Green Chem. 19 (2017) 3692-3706.
[10] M. Hong, E.Y.X. Chen, Trends Chem. 1 (2019) 148-151.
[11] X. Tang, E.Y.X. Chen, Chem 5 (2019) 284-312.
[12] G.W. Coates, Y.D.Y.L. Getzler, Nat. Rev. Mater. 5 (2020) 501-516.
[13] C. Shi, M.L. McGraw, Z.C. Li, et al., Sci. Adv. 6 (2020) eabc0495.
[14] C. Shi, Z.C. Li, L. Caporaso, et al., Chem 7 (2021) 670-685.
[15] C. Shi, L.T. Reilly, V.S. Phani Kumar, et al., Chem 7 (2021) 2896-2912.
[16] C. Shi, R.W. Clarke, M.L. McGraw, et al., J. Am. Chem. Soc. 144 (2022) 2264-2275.
[17] G. Xu, Q. Wang, Green Chem. 24 (2022) 2321-2346.
[18] C.M. Plummer, L. Li, Y. Chen, Macromolecules 56 (2023) 731-750.
[19] C. Shi, W.T. Diment, E.Y.X. Chen, Angew. Chem. Int. Ed. 63 (2024) e202405083.
[20] C. Shi, N.A. Rorrer, A.L. Shaw, et al., J. Am. Chem. Soc. 146 (2024) 9261-9271.
[21] Y. Sun, Z. An, Y. Gao, et al., Sci. China Chem. 67 (2024) 2803-2841.
[22] C. Shi, E.C. Quinn, W.T. Diment, et al., Chem. Rev. 124 (2024) 4393-4478.
[23] F. Vidal, E.R. van der Marel, R.W.F. Kerr, et al., Nature 626 (2024) 45-57.
[24] Q.Z. Guo, Y. Du, J.F. Guo, et al., Chin. Chem. Lett. 24 (2013) 897-900.
[25] C.V. Aarsen, A. Liguori, R. Mattsson, et al., Chem. Rev. 124 (2024) 8473-8515.
[26] X. Liu, J. Yang, Z. He, et al., Chin. Chem. Lett. 36 (2025) 110236.
[27] Y. Xia, C. Zhang, Y. Wang, et al., Chin. Chem. Lett. 35 (2024) 108860.
[28] D.K. Schneiderman, M.A. Hillmyer, Macromolecules 50 (2017) 3733-3749.
[29] X.B. Lu, Y. Liu, H. Zhou, Chemistry 24 (2018) 11255-11266.
[30] X. Zhang, M. Fevre, G.O. Jones, et al., Chem. Rev. 118 (2018) 839-885.
[31] Z. Wang, M.S. Ganewatta, C. Tang, Prog. Polym. Sci. 101 (2020) 101145.
[32] R.M. Cywar, N.A. Rorrer, C.B. Hoyt, et al., Nat. Rev. Mater. 7 (2021) 83-103.
[33] Q. Zhang, M. Song, Y. Xu, et al., Prog. Polym. Sci. 120 (2021) 101430.
[34] C. Shi, L.T. Reilly, E.Y.X. Chen, Angew. Chem. Int. Ed. 62 (2023) e202301850.
[35] C. Shi, Z. Zhang, M. Scoti, et al., ChemSusChem 16 (2023) e202300008.
[36] X.B. Meng, T. Zhou, C. Yang, et al., J. Am. Chem. Soc. 146 (2024) 15428-15437.
[37] C. Shi, Y. Ge, E.Y.X. Chen, One Earth 8 (2025) 101517.
[38] M. Antar, D. Lyu, M. Nazari, et al., Renew. Sustain. Energy Rev. 139 (2021) 110691.
[39] V.G. Matveeva, L.M. Bronstein, Prog. Mater Sci. 130 (2022) 100999.
[40] J.G. Rosenboom, R. Langer, G. Traverso, Nat Rev Mater 7 (2022) 117-137.
[41] K. Sanderson, Nature 474 (2011) S12-S14.
[42] I. Itabaiana Junior, M. Avelar do Nascimento, R.O.M.A. de Souza, et al., Green Chem. 22 (2020) 5859-5880.
[43] Y. Zhao, Y. Li, Q. An, et al., Chin. Chem. Lett. (2025), https://doi.org/10.1016/j.cclet.2025.112357.
[44] M.K. Stanfield, R.S. Terry, J.A. Smith, et al., Polym. Chem. 14 (2023) 4949-4956.
[45] M.B. Comba, Y. Tsai, A.M. Sarotti, et al., Eur. J. Org. Chem. 2018 (2018) 590-604.
[46] J.E. Camp, B.W. Greatrex, Front Chem 10 (2022) 902239.
[47] C.M. Warne, S. Fadlallah, A.C. Whitwood, et al., Green Chem. Lett. Rev. 16 (2022) 2154573.
[48] C.B.T.L. Lee, T.Y. Wu, Renewable Sustain. Energy Rev. 137 (2021) 110172.
[49] F. Allais, Curr. Opin. Green Sustain. Chem. 40 (2023) 100744.
[50] S. Fadlallah, L.M.M. Mouterde, G. Garnier, et al., in: A.M. Peru, S. Fadlallah (Eds.), Sustainability & Green Polymer Chemistry Volume 2: Biocatalysis and Biobased Polymers, American Chemical Society, Washington, DC, 2020, pp. 77-97.

[51] O.J. Lamb, H. Podversnik, J. Puschnig, et al., ChemistrySelect 11 (2026) e07470.
[52] E.T. Ledingham, B.W. Greatrex, Tetrahedron 74 (2018) 6107-6115.
[53] E.T. Ledingham, K.P. Stockton, B.W. Greatrex, Aust. J. Chem. 70 (2017) 1146-1150.
[54] C.M. Pacheco, W. Lima, F.A. Lima, et al., RSC Adv. 14 (2024) 34611-34619.
[55] V. Mamleev, S. Bourbigot, M. Le Bras, et al., J. Anal. Appl. Pyrolysis 84 (2009) 1-17.
[56] X. Zhang, W. Yang, C. Dong, J. Anal. Appl. Pyrolysis 104 (2013) 19-27.
[57] S. Kudo, N. Goto, J. Sperry, et al., ACS Sustain. Chem. Eng. 5 (2017) 1132-1140.
[58] J. He, M. Liu, K. Huang, et al., Green Chem. 19 (2017) 3642-3653.
[59] B. Hu, Q. Lu, Y. Wu, et al., J. Energy Chem. 43 (2020) 78-89.
[60] S.H. Krishna, T.W. Walker, J.A. Dumesic, et al., ChemSusChem 10 (2017) 129-138.
[61] S. Li, S. Li, C. Wang, et al., Fuel Process. Technol. 209 (2020) 106525.
[62] Y. Li, B. Hu, H. Fu, et al., Energy Fuels 36 (2022) 10251-10260.
[63] X. Meng, H. Zhang, C. Liu, et al., Energy Fuels 30 (2016) 8369-8376.
[64] O. Oyola-Rivera, J. He, G.W. Huber, et al., Biomass Bioenergy 156 (2022) 106315.
[65] S. Saragai, S. Kudo, J. Sperry, et al., Bioresour. Technol. 344 (2022) 126323.
[66] B. Wang, K. Li, C. Zhang, et al., Ind. Crops Prod. 192 (2023) 116072.
[67] B. Wang, K. Li, C. Zhang, et al., Ind. Crops Prod. 206 (2023) 117594.
[68] A. Xu, X. Huang, G. Tang, et al., Fuel Process. Technol. 242 (2023) 107609.
[69] H. Yang, S. Lei, K. Xu, et al., Fuel Process. Technol. 234 (2022) 107323.
[70] H. Zhang, X. Meng, C. Liu, et al., Fuel Process. Technol. 167 (2017) 484-490.
[71] S. Kudo, X. Huang, S. Asano, et al., Energy Fuels 35 (2021) 9809-9824.
[72] Y. Halpern, R. Riffer, A. Broido, J. Org. Chem. 38 (1973) 204-209.
[73] F. Shafizadeh, P.P.S. Chin, Carbohydr. Res. 58 (1977) 79-87.
[74] M. Shibagaki, K. Takahashi, H. Kuno, et al., Chem. Lett. 19 (1990) 307-310.
[75] F.D. Bobbink, Z. Huang, F. Menoud, et al., ChemSusChem 12 (2019) 1437-1442.
[76] T. Taniguchi, K. Nakamura, K. Ogasawara, Synlett 1996 (1996) 971-972.
[77] F. Cao, T.J. Schwartz, D.J. McClelland, et al., Energy Environ. Sci. 8 (2015) 1808-1815.
[78] Q. Cao, T. Ye, W. Li, et al., Cellulose 27 (2020) 9825-9838.
[79] F. Xu, J. Luo, L. Jiang, et al., Cellulose 29 (2022) 1463-1472.
[80] X. Ye, Q. Lu, X. Wang, et al., ACS Sustain. Chem. Eng. 5 (2017) 10815-10825.
[81] K. Li, B. Wang, D. Bolatibieke, et al., J. Anal. Appl. Pyrolysis 148 (2020) 104824.
[82] D. Fabbri, C. Torri, I. Mancini, Green Chem. 9 (2007) 1374-1379.
[83] L. Qian, F. Xu, S. Liu, et al., Cellulose 28 (2021) 7579-7592.
[84] S. Kudo, Z. Zhou, K. Norinaga, et al., Green Chem. 13 (2011) 3306-3311.
[85] A. Doroshenko, I. Pylypenko, K. Heaton, et al., ChemSusChem 12 (2019) 5224-5227.
[86] L. A, H. Radhakrishnan, H. Hu, et al., Green Chem. 22 (2020) 7871-7883.
[87] N.A. Stini, P.L. Gkizis, C.G. Kokotos, Green Chem. 24 (2022) 6435-6449.
[88] B. Pollard, M.G. Gardiner, M.G. Banwell, et al., ChemSusChem 17 (2024) e202301165.
[89] T. Debsharma, F.N. Behrendt, A. Laschewsky, et al., Angew. Chem. Int. Ed. 58 (2019) 6718-6721.
[90] T. Debsharma, B. Schmidt, A. Laschewsky, et al., Macromolecules 54 (2021) 2720-2728.
[91] S. Fadlallah, A.A.M. Peru, A.L. Flourat, et al., Eur. Polym. J. 138 (2020) 109980.
[92] S. Fadlallah, A.A.M. Peru, L. Longé, et al., Polym. Chem. 11 (2020) 7471-7475.
[93] M.G. Banwell, X. Liu, L.A. Connal, et al., Macromolecules 53 (2020) 5308-5314.
[94] E. Jung, A. Rizzo, H. Ryu, et al., Chem. Sci. 16 (2025) 8435-8442.
[95] A.B. Pabarue, X. Sui, Y. Bu, et al., J. Polym Sci. 63 (2025) 2349-2355.
[96] T. Debsharma, Y. Yagci, H. Schlaad, Angew. Chem. Int. Ed. 58 (2019) 18492-18495.
[97] K. Kaya, T. Debsharma, H. Schlaad, et al., Polym. Chem. 11 (2020) 6884-6889.
[98] M.K. Porwal, C.J. Ellison, T.M. Reineke, ACS Macro Lett. 12 (2023) 935-942.
[99] L. Wu, Z. Zhou, D. Sathe, et al., Nat. Chem. 15 (2023) 1276-1284.
[100] Y. Mizukami, Y. Kakehi, F. Li, et al., ACS Macro Lett. 13 (2024) 252-259.
[101] H. Meng, H. Chen, B. Hu, et al., ChemCatChem 17 (2025) e00889.
[102] H.C. Sheers, M.K. Stanfield, J.A. Smith, et al., Polym. Chem. 16 (2025) 5093-5105.
[103] G. Tang, X. Huang, A. Xu, et al., Ind. Crops Prod. 189 (2022) 115777.
[104] P. Ray, T. Hughes, C. Smith, et al., ACS Omega 3 (2018) 2040-2048.
[105] P. Ray, T. Hughes, C. Smith, et al., Polym. Chem. 10 (2019) 3334-3341.
[106] L. Wu, H. Kim, T.L. Choi, J. Am. Chem. Soc. 147 (2025) 11682-11687.
[107] C. Paris, M. Moliner, A. Corma, Green Chem. 15 (2013) 2101-2109.
[108] A.L. Flourat, A.A.M. Peru, A.R.S. Teixeira, et al., Green Chem. 17 (2015) 404-412.
[109] G. Bonneau, A.A.M. Peru, A.L. Flourat, et al., Green Chem. 20 (2018) 2455-2458.
[110] F. Shafizadeh, R.H. Furneaux, D. Pang, et al., Carbohydr. Res. 100 (1982) 303-313.
[111] F. Diot-Néant, L. Mouterde, S. Fadlallah, et al., ChemSusChem 13 (2020) 2613-2620.
[112] F. Diot-Néant, L.M.M. Mouterde, C. Veith, et al., ACS Sustain. Chem. Eng. 10 (2022) 10132-10143.
[113] F. Diot-Néant, L.M.M. Mouterde, J. Couvreur, et al., Eur. Polym. J. 159 (2021) 110938.
[114] A. Kayishaer, S. Fadlallah, L.M.M. Mouterde, et al., Molecules 26 (2021) 7672.
[115] A. Tahara, S. Yashiro, T. Hokajo, et al., Polym. Chem. 16 (2024) 800-808.
[116] M.K. Porwal, M.M. Hausladen, C.J. Ellison, et al., Green Chem. 25 (2023) 1488-1502.
[117] M.P. Timilsina, M.K. Stanfield, J.A. Smith, et al., ChemPlusChem 89 (2024) e202400383.

Graphical Abstract

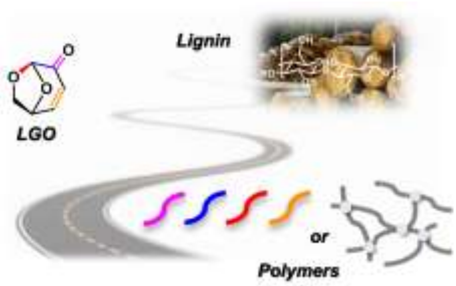

Levoglucosenone, a chiral platform molecule obtained from cellulose pyrolysis, enables the design of diverse sustainable polymers through tailored functionalization and polymerization strategies, bridging renewable carbon and circular materials.

Declaration of Interest Statement

☒ The authors declare that they have no known competing financial interests or personal relationships that could have appeared to influence the work reported in this paper.

☐ The author is an Editorial Board Member/Editor-in-Chief/Associate Editor/Guest Editor for this journal and was not involved in the editorial review or the decision to publish this article.

☐ The authors declare the following financial interests/personal relationships which may be considered as potential competing interests: